Available online at www.sciencedirect.com
SCIENCE DIRECT
Journal of Catalysis 241 (2006) 180–188
JOURNAL OF CATALYSIS
www.elsevier.com/locate/jcat

On the structure and composition of the phosphosulfide overlayer on Ni_2P at hydrotreating conditions

Alan E. Nelson *, Mingyong Sun, Abu S.M. Junaid

University of Alberta, Department of Chemical and Materials Engineering, Edmonton, Alberta, Canada T6G 2G6

Received 16 February 2006; revised 6 April 2006; accepted 8 April 2006

Abstract

Ni_2P has shown very promising catalytic activity as a hydrotreating catalyst, but the exact structure of the actual active phase is not understood. The present work has systematically studied the structures and energetics of possible surface compositions of the (001) surface of Ni_2P (i.e., the Ni_3P_2 plane) at hydrotreating conditions using density functional theory calculations. By comparing the energetics of surfaces with adsorbed H_2S, –SH, and atomic sulfur and the surfaces with phosphorous replaced by sulfur as a function of concentration and atomic location on the (001) surface, we have identified a stable phosphosulfide surface consistent with a surface stoichiometry of Ni_3PS. This surface composition is energetically more stable than bulk Ni_2P or Ni_3S_2 at hydrotreating conditions. To provide additional confirmation of the proposed surface structure, we calculated CO absorbance frequencies on the Ni_3P_2 and Ni_3PS surfaces as a function of surface CO coverage, and found that they are in excellent agreement with previously published experimental infrared spectroscopy data. These calculations, combined with literature experimental observations, indicate that the surface with 50% phosphorus replaced by sulfur and some atomic sulfur deposited on the three-fold hollow sites is an accurate representation for the actual active phase, or the so-called "phosphosulfide" surface, of Ni_2P at typical hydrotreating conditions.

Keywords: Nickel phosphide; Ni_2P; Hydrotreating; DFT; CO adsorption; IR spectroscopy; Phosphosulfide

1. Introduction

The increasing use of highly contaminated heavy oils and increasingly stringent environmental regulations have made catalytic hydrotreating of paramount importance to the petroleum industry. Traditional hydrotreating catalysts are nickel- (or cobalt-) promoted molybdenum (or tungsten) sulfides supported on high-surface area γ-alumina [i.e., Ni(Co)–Mo(W)/γ-Al_2O_3], which often contain phosphorous as a secondary promoter. During the past two decades, significant effort has been made to understand and improve these classic sulfide-based catalysts [1–8]. Recently, significant attention has been given to searching for new materials as hydrotreating catalysts, and many studies have identified transition metal phosphides as promising materials for novel hydrotreating catalysts [9–20]. Of the transition metal phosphides studied to date, Ni_2P has been shown to have high hydrotreating activity and good stability [15,17–20]. These studies follow on the earlier observation of Robinson et al. [21], who attributed the activity of supported phosphorous-promoted hydrotreating catalysts to the presence of Ni_2P.

The stability of phosphide catalysts against sulfidation at hydrotreating conditions has been of concern, potentially limiting the industrial application of these catalysts. It was previously reported that Ni_2P irreversibly lost some of its intrinsic HDN activity after exposure to H_2S over time [10,20]. Bussell et al. [11,18] and Oyama et al. [13,15,17] tested the HDS activity of Ni_2P catalysts for more than 100 h, and although they found no significant deactivation, EXAFS analysis of Ni_2P catalyst showed the formation of Ni–S bonds after HDS reactions [13, 15,17]. However, XRD measurements of samples before and after HDS reactions did not reveal significant changes in the bulk structure of Ni_2P [13,15,17]. Studies with infrared spectroscopy of CO adsorbed on Ni_2P catalysts after sulfidation also indicated that the surface of Ni_2P might be partially sulfided

* Corresponding author. Fax: +1 780 492 2881.
E-mail address: alan.nelson@ualberta.ca (A.E. Nelson).

0021-9517/$ – see front matter
doi:10.1016/j.jcat.2006.04.023

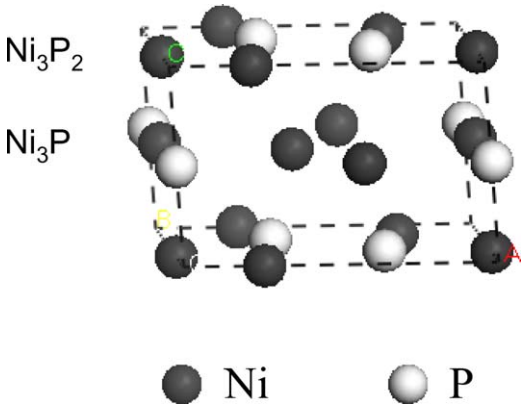

Fig. 1. Unit cell of bulk Ni_2P.

[18,19]. These results suggest that a phosphosulfide overlayer might have formed on the surface of a Ni_2P core during hydrotreating, suggesting the active phase may be a phosphosulfide and not a phosphide phase or a sulfide phase, but the exact structure of the phosphosulfide overlayer is not clear. In addition, several studies have reported the hydrotreating activity of Ni(Co)–P(S) model compounds [21,22]. One of the compounds studied, $NiPS_3$, exhibited minor catalytic activity and converted to Ni_2P during pretreatment or reaction [21]. The characterization of fresh $NiPS_3$ by X-ray photoelectron spectroscopy (XPS) indicated the presence of a type of "PS" compound similar to Ph_3PS; but after sulfidation, this compound disappeared from the spectra [22].

The present work uses density functional theory (DFT) to examine possible structures for the phosphosulfide overlayer on the $Ni_2P(001)$ surface resulting from H_2S adsorption and dissociation, as well as the replacement of surface phosphorus by sulfur. The relative stabilities of different structures are considered and evaluated at hydrotreating conditions. In addition, the energetics and frequencies of CO adsorption are used to further characterize the surface structure in comparison with infrared spectroscopy (IR) data available in the literature. A surface compositional model is subsequently presented to describe the structure of the phosphosulfide overlayer on Ni_2P and is shown to be in excellent agreement with previous experimental observations.

2. Methods

2.1. Structural models

The unit cell of bulk Ni_2P was built based on crystallographic data [23] and subsequently geometrically optimized (i.e., energy minimization) to further refine the structural model. Along the (001) direction of Ni_2P, two types of planes with Ni_3P_2 and Ni_3P compositions alternate, as shown in Fig. 1. A recently published STM study provides direct experimental evidence for the existence of these Ni_3P- and Ni_3P_2-terminated surfaces on Ni_2P single crystals [24]. The surface free energies of the (001) planes with different terminations were calculated, and the surface free energy of the Ni_3P_2 termination was found to be 0.021 eV/Å^2 lower than that of Ni_3P. This is consistent with previous results [25]. Therefore, we used the Ni_3P_2 plane to represent the (001) surface of Ni_2P. Fig. 2 shows the periodic models used in the present work. These surface models consist of four layers of Ni and P atoms, along with a 15-Å vacuum layer in the z-direction (Fig. 2A). Both the supercell

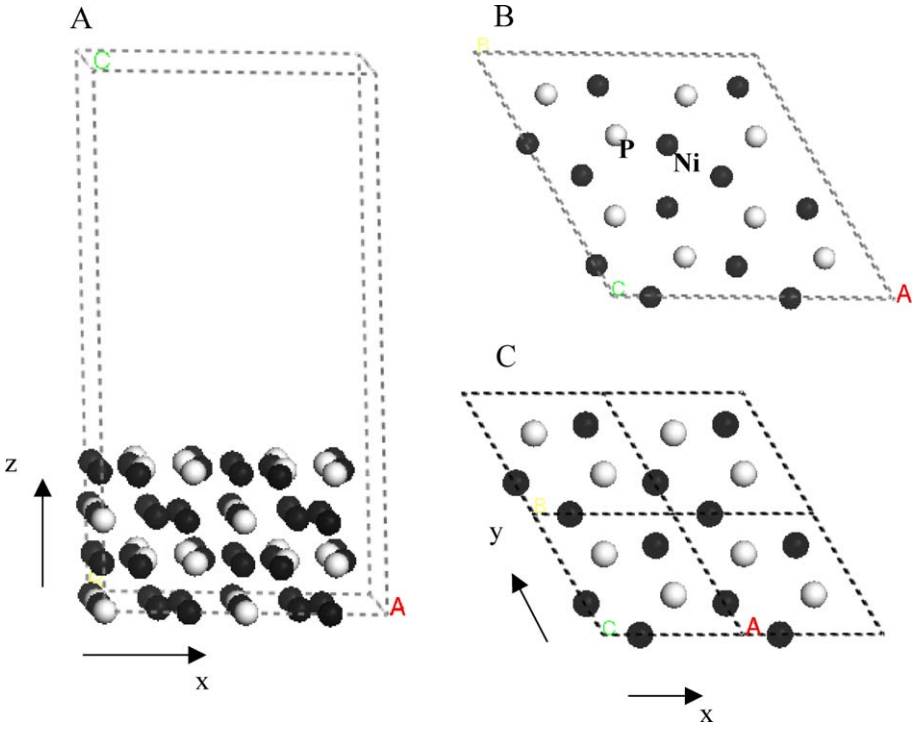

Fig. 2. Periodic models of $Ni_2P(001)$ surface; (A) side view showing the four-layered catalyst slab and 15 Å vacuum layer, (B) top view of the supercell including four units of Ni_3P_2, and (C) top view of the unitcell including one unit of Ni_3P_2.

(Fig. 2B) and unit cell (Fig. 2C) models were used to represent the Ni_3P_2-terminated (001) surface of Ni_2P.

2.2. DFT calculations

The calculations are based on DFT and performed using MS Modeling DMol^3 from Accelrys® (version 3.2) [26]. The double-numerical plus polarization (DNP) functions and Becke exchange [27] plus Perdew–Wang approximation [28] nonlocal functionals (GGA-PW91) are used in all calculations. The real space cutoff radius is 4.5 Å. All electron basis sets are used for light elements, such as hydrogen, carbon, oxygen, phosphorus, and sulfur. Effective core potentials [29,30] are used to treat core electrons of nickel. The *k-point* set of $(1 \times 1 \times 1)$ is used for supercell calculations, and $(4 \times 4 \times 1)$ is used for unit cell calculations. Spin polarization is applied to all calculations. The parameters used in this study have been checked for convergence with an accuracy of total energy <0.01 eV and of vibrational frequency $<10\ \mathrm{cm}^{-1}$.

2.3. Thermodynamic calculations

Relative energies of the surfaces with different sulfur species are calculated according to similar methods previously used for sulfide catalysts [3,31–33]. Briefly, for a free H_2S molecule plus a clean Ni_2P surface, the energy changes for molecular adsorption, dissociation to –SH plus gas-phase hydrogen, and dissociation to adsorbed sulfur plus gas-phase hydrogen are calculated using the following equations:

$$\Delta E_{H_2S} = E(H_2S \text{ adsorbed surface}) - E(\text{clean surface}) - E(\text{free } H_2S), \quad (1)$$

$$\Delta E_{HS} = E(\text{HS adsorbed surface}) + \frac{1}{2}E(\text{free } H_2) - E(\text{clean surface}) - E(\text{free } H_2S), \quad (2)$$

$$\Delta E_S = E(\text{sulfur adsorbed surface}) + E(\text{free } H_2) - E(\text{clean surface}) - E(\text{free } H_2S). \quad (3)$$

Considering the temperature corrections and pressure effects, the free energy changes for corresponding processes are calculated as follows:

$$\Delta G_{H_2S} = \Delta E_{H_2S} + \Delta G^0_{T_{corr}} - RT \ln p_{H_2S}, \quad (4)$$

$$\Delta G_{HS} = \Delta E_{HS} + \Delta G^0_{T_{corr}} + \frac{1}{2}RT \ln p_{H_2} - RT \ln p_{H_2S}, \quad (5)$$

$$\Delta G_S = \Delta E_S + \Delta G^0_{T_{corr}} - RT \ln \frac{p_{H_2S}}{p_{H_2}}. \quad (6)$$

In addition to the adsorption and dissociation of H_2S on the Ni_2P surface, surface phosphorus also may be replaced by sulfur to form a partially sulfided surface. The phosphorus released from Ni_2P catalyst can be in the form of PH_3 or elemental phosphorus depending on reaction conditions. Oyama et al. detected PH_3 production during the temperature-programmed reduction (TPR) of their catalyst precursor [17]. Thus, in the discussions of the relative stability of different structures, we take PH_3, H_2S, and H_2 as energetic references. The electronic and free energy changes for sulfur-replacing surface phosphorus can be calculated by the following:

$$\Delta E_{Ni_3PS} = E(Ni_3PS \text{ surface}) + E(PH_3) - E(Ni_3P_2 \text{ surface}) - E(H_2S) - \frac{1}{2}E(H_2), \quad (7)$$

$$\Delta G_{Ni_3PS} = \Delta E_{Ni_3PS} + \Delta G^0_{T_{corr}} + RT\left(\ln p_{PH_3} - \frac{1}{2}\ln p_{H_2} - \ln p_{H_2S}\right). \quad (8)$$

The electronic and free energy changes for full sulfidation of bulk Ni_2P to bulk Ni_3S_2 are calculated as follows:

$$\Delta E_{Ni_3S_2} = \frac{2}{3}E(Ni_3S_2) + E(PH_3) - E(Ni_2P) - \frac{4}{3}E(H_2S) - \frac{1}{6}E(H_2), \quad (9)$$

$$\Delta G_{Sulfidation} = \Delta E_{Sulfidation} + \Delta G^0_{T_{corr}} + RT\left(\ln p_{PH_3} - \frac{1}{6}\ln p_{H_2} - \frac{4}{3}\ln p_{H_2S}\right). \quad (10)$$

In the calculations of free energy changes, the electronic energy changes are corrected to include enthalpy changes and entropy changes for gas-phase molecules at reaction temperatures expressed by $\Delta G^0_{T_{corr}}$ in Eqs. (4)–(6), (8), and (10).

3. Results and discussion

3.1. Adsorption and dissociation of H_2S on the Ni_2P surface

Different initial configurations for H_2S adsorption on the Ni_2P surface are considered to find the optimized structure with the minimum energy. When the sulfur atom of H_2S is placed between a phosphorus atom and a nickel atom, the sulfur atom migrates to atop the nickel atom during geometry optimization. When the sulfur atom of H_2S is on the top of a nickel atom, the two hydrogen atoms prefer to point toward the two neighbor nickel atoms rather than to the two neighbor phosphorus atoms. Fig. 3A presents the most stable configuration for H_2S adsorption on the Ni_2P surface; the adsorption energy calculated according to Eq. (1) is -0.75 eV/H_2S.

In addition to molecular adsorption, the possibility of the adsorbed H_2S dissociating to adsorbed atomic hydrogen and sulfur is also considered. When the two hydrogen atoms and the sulfur atoms are placed on three neighbor nickel atoms that form a three-fold hollow (TFH), the two hydrogen atoms combine with the sulfur atom to form an adsorbed H_2S similar to that shown in Fig. 3A. Another possibility for H_2S dissociation is the formation of adsorbed –SH or an adsorbed sulfur atom plus gas-phase hydrogen. For adsorbed –SH, the sulfur atom bridges two of the three trigonal nickel atoms, and the hydrogen atom is located atop the other nickel atom, as shown in Fig. 3B. The sulfur atom forms two shorter bonds (2.26 Å) with the bridged nickel atoms and one longer bond (2.51 Å) with the third nickel atom; the hydrogen atom does not form a bond with any nickel atoms. The adsorption energy calculated according to Eq. (2) is -1.48 eV/H_2S.

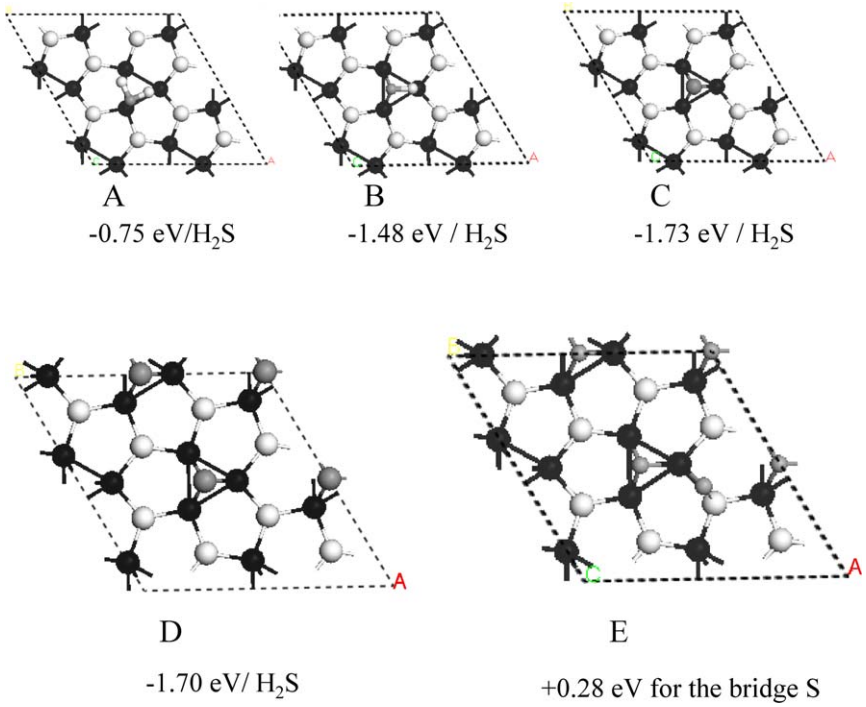

Fig. 3. The structures and energetics for H_2S adsorption and dissociation on the $Ni_2P(001)$ surface. (A) H_2S molecule adsorbed, (B) H_2S dissociated to an adsorbed –SH and one-half gas phase H_2, (C) H_2S dissociated to an adsorbed sulfur atom and a free H_2, (D) H_2S adsorption and dissociation on all TFH sites, and (E) additional H_2S adsorption and dissociation on a Ni–P bridge site. The energy data are relative to a clean surface and gas-phase H_2S and H_2.

The dissociation can proceed to form an adsorbed sulfur atom and gas-phase hydrogen. The adsorbed sulfur atom prefers the center of a TFH site, as shown in Fig. 3C. The adsorption energy calculated according to Eq. (3) is -1.73 eV/H_2S. The adsorption of one sulfur atom on one TFH site does not affect the adsorption of sulfur atoms on other TFH sites. The total adsorption energy increases linearly with the number of sulfur atoms until all TFH sites are covered by sulfur adatoms (Fig. 3D). After all TFH sites are occupied, the adsorption energy of an additional sulfur atom on a Ni–P bridge site is $+0.28$ eV (Fig. 3E). Adding additional sulfur atoms on the TFH-filled surface is always an endothermic process.

The free energy changes for the foregoing three adsorption and dissociation processes at temperature T, p_{H_2S}, and p_{H_2} can be calculated by Eqs. (4)–(6), respectively. Fig. 4 shows the free energy changes as a function of temperature at a hydrogen pressure of 5.0 MPa and H_2S pressure of 0.1 MPa, which are typical conditions for hydrotreating. Negative ΔG values indicate that the structures with sulfur on the surface are more stable than a clean Ni_2P surface with free H_2S molecules in the gas phase. The relative stability at low temperature increases in the following order: free H_2S + Ni_2P clean surface < adsorbed H_2S on Ni_2P surface < adsorbed –SH + one-half free hydrogen molecule < adsorbed sulfur atom + free hydrogen molecule. At high temperatures, molecularly adsorbed H_2S becomes less stable than gas-phase H_2S and it will desorb from the surface, but the dissociated sulfur species, –SH, and sulfur adatoms are stable on the surface up to 1000 K at these hydrotreating pressures.

The actual populations of these three types of sulfur on the surface depend on the reaction conditions and kinetics of H_2S dissociation, as well as the hydrogenation of adsorbed sulfur. Normally, adsorption of H_2S on the catalyst surface can readily occur without significant activation energy. If the sulfur stays on the surface in the form of molecularly adsorbed H_2S, then the H_2S is stable on the surface up to about 550 K at 0.1 MPa H_2S partial pressure. Reducing H_2S partial pressure will lower the temperature, and increasing H_2S partial pressure will increase the temperature required for removing H_2S from the surface. An approximate 10-fold increase in H_2S partial pressure requires an approximately 50 K higher desorption temperature.

If the adsorbed H_2S can overcome the activation energy required to dissociate to adsorbed –SH or a sulfur adatom, then the sulfur species is further stabilized on the catalyst surface. In the presence of 0.1 MPa H_2S, adsorbed –SH or a sulfur atom cannot be removed from the surface at 5.0 MPa, even at 1000 K (Fig. 4). When the H_2S concentration in the gas phase is reduced to a very low level, all of the sulfur species can be desorbed at a reasonable temperature range. For example, when the H_2S concentration is reduced to 0.1 ppm in 5.0 MPa hydrogen, the adsorbed –SH and sulfur atoms can be removed from the surface at 650 and 850 K, respectively.

Liu et al. observed that on the $Ni_2P(001)$ surface, some sulfur species were stable up to 700 K, and that some others desorb at about 400–450 K under ultra-high-vacuum (UHV) atmosphere [25]. They attributed the weakly bonded sulfur species to sulfur atoms adsorbed on the Ni–P bridge sites and the strongly bonded sulfur species to sulfur atoms on the TFH sites. They also calculated the adsorption energy of sulfur atoms on the TFH site and on a Ni–P bridge site. Their data indicated that the adsorption of a sulfur atom on the Ni–P bridge site af-

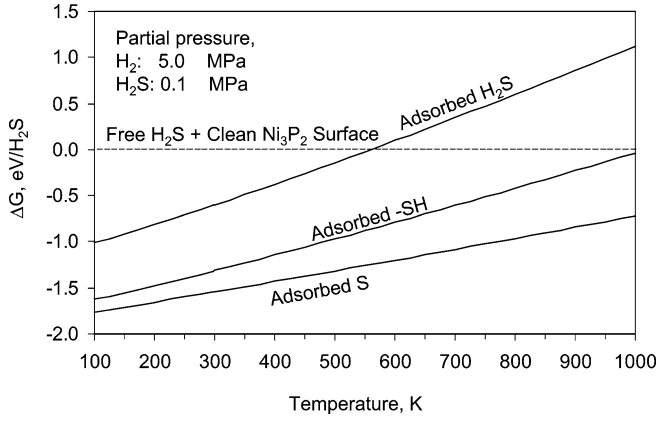

Fig. 4. Free energy changes for the adsorption and dissociation of H_2S on the $Ni_2P(001)$ surface as a function of temperature at 5.0 MPa hydrogen and 0.1 MPa H_2S. The pristine Ni_3P_2 surface and gas-phase H_2S and H_2 are taken as energetic references.

ter the TFH site is occupied is actually an endothermic process. Therefore, the bridge sulfur atom is unlikely to be present on the surface in significant quantities. Based on these results, the weakly bonded sulfur species that desorb at 400–450 K in the XPS experiment are likely nondissociated H_2S, and the strongly bonded sulfur species that desorb above 700 K in UHV atmosphere are the sulfur atoms adsorbed on the TFH sites.

3.2. Surface phosphorus replacement by sulfur

In addition to the adsorption and dissociation of H_2S on the Ni_2P surface, it is also possible that hydrogen can react with surface phosphorus to form PH_3, thereby creating phosphorus-defect sites. H_2S would then adsorb and dissociate on the defect sites. The energy required to remove a phosphorus atom from the Ni_3P_2 supercell surface is +1.71 eV (Fig. 5, from A to B). The free energy change for this step is negative at approximately 750 K when the Ni_2P catalyst is reduced with 100 kPa of fresh hydrogen with a PH_3 partial pressure $<1 \times 10^{-7}$ Pa. Normally, Ni_2P catalysts are prepared by reducing the phosphate precursor in a hydrogen flow up to 850–923 K [17,18]. Therefore, it is possible to generate some surface P-defect sites.

Once the defect site is formed, it is very active. H_2S spontaneously dissociates to an adsorbed –SH group and atomic hydrogen during geometry optimization of H_2S on the defect site (Fig. 5C). The dissociative adsorption energy of H_2S on the defect site is −2.36 eV. An additional 0.33 eV is required to remove the hydrogen atoms from the surface as a free hydrogen molecule and leave a sulfur atom on the defect site (Fig. 5D). The overall reaction from A to D is the replacement of phosphorus by sulfur on the Ni_3P_2 plane of the $Ni_2P(001)$ surface. The net energy change for this overall process is −0.32 eV.

Replacing a second phosphorus atom that shares one nickel atom with the first sulfur atom is much less exothermic, with an energy change of approximately −0.1 eV. However, if the second phosphorus atom is apart from the sulfur (i.e., does not share a nickel atom with the sulfur atom), then the additional energy change will be approximately −0.30 eV. This indicates that the initial sulfur inhibits additional replacement of phosphorus locally, but does not affect the replacement of other phosphorus atoms apart from the sulfur atom. The overall sulfur replacement process continues to be exothermic until 50% of surface phosphorus atoms are replaced, as shown in Fig. 6A. Replacing an additional phosphorus atom from the 50% phosphorus-replaced surface to obtain 62.5% phosphorous replacement (Fig. 6B) is an endothermic process (+0.30 eV/S). The replacement of an additional phosphorus atom from the sublayer of the 50% phosphorus-replaced surface (Fig. 6C) is

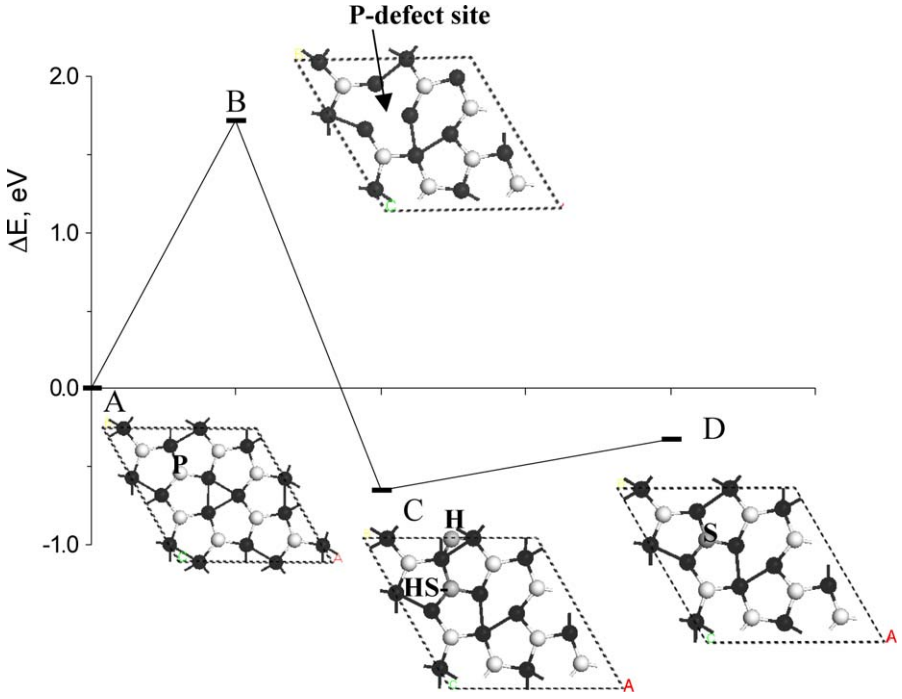

Fig. 5. Energy profile for phosphorous-defect formation, and H_2S adsorption and dissociation on the defect site.

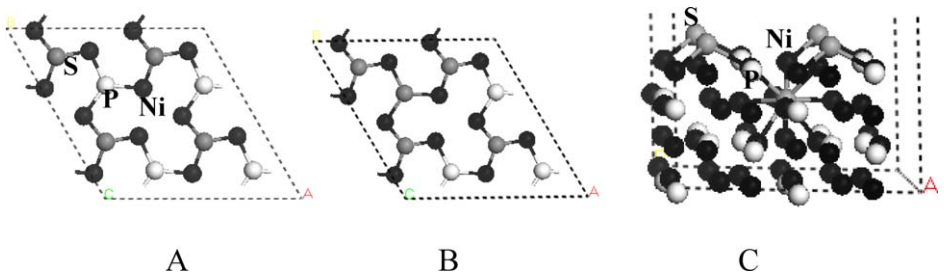

Fig. 6. Top views of, (A) the 50% sulfur replaced, (B) the 62.5% sulfur replacement $Ni_2P(001)$ surface, and (C) side view of 50% sulfur replacement $Ni_2P(001)$ surface with an additional sublayer phosphorus replaced by sulfur.

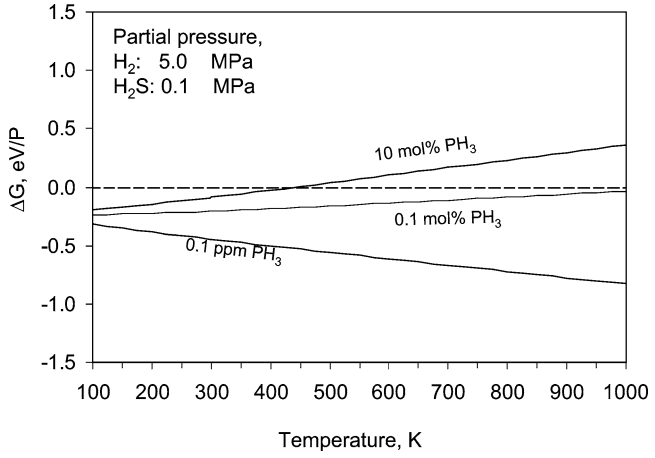

Fig. 7. Free energy changes for the replacement of 50% phosphorus by sulfur from the (001) surface of Ni_2P as a function of temperature at 5.0 MPa hydrogen and 0.1 MPa H_2S. The pristine Ni_3P_2 surface and gas phase H_2S and H_2 are taken as energetic references.

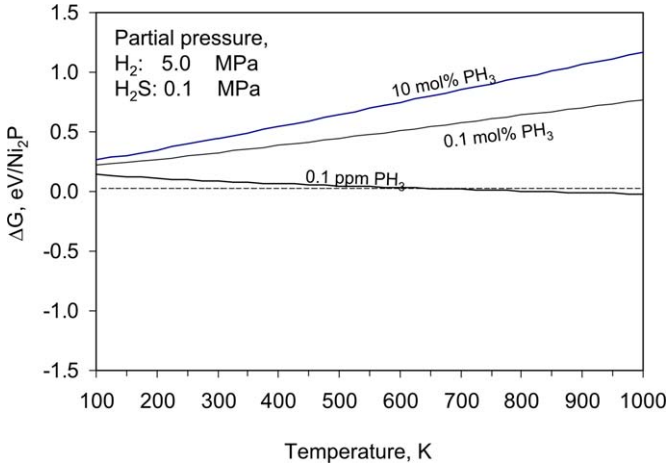

Fig. 8. Free energy changes for the complete sulfidation of Ni_2P to Ni_3S_2 as a function of temperature at 5.0 MPa hydrogen and 0.1 MPa H_2S with different PH_3 concentrations in the gas phase.

highly endothermic with $\Delta E = +1.29$ eV. Therefore, the 50% phosphorus-replaced surface is the most stable structure for the sulfur replacement model (Fig. 6A).

According to the stoichiometry of the surface composition, the 50% phosphorus-replaced surface is represented by Ni_3PS. The relative stability of the Ni_3PS surface against the pristine Ni_3P_2 surface of Ni_2P depends on reaction conditions. Fig. 7 shows the relative free energy of the Ni_3PS relative to the pristine Ni_3P_2 surface as a function of temperature at 5.0 MPa hydrogen and 0.1 MPa H_2S calculated by Eq. (8). When the concentration of PH_3 in the gas phase is about 10 mol%, the pristine Ni_3P_2 surface is more stable than the Ni_3PS surface at high temperatures (>450 K). At a lower concentration of PH_3 (but >0.1 mol%) in the gas phase, higher temperatures are required to prevent phosphorus on the Ni_3P_2 surface from being replaced by sulfur. However, at very low concentrations of PH_3 (<0.1 mol%), the partially sulfided Ni_3PS surface is always more stable than the pristine Ni_3P_2 surface (Fig. 7). At normal hydrotreating conditions, if no additional phosphorus is added to the reactor, then 50% surface phosphorus will be gradually replaced by sulfur to form a phosphosulfide overlayer on the surface of Ni_2P.

In addition, the possibility of complete sulfidation of bulk Ni_2P to bulk Ni_3S_2 at relevant conditions was also studied. The relative stability of Ni_3S_2 relative to Ni_2P is determined by the free energy change of converting Ni_2P to Ni_3S_2 in the presence of H_2S and hydrogen at high temperatures, as calculated by Eq. (10). Fig. 8 presents the temperature dependence of the free energy change for complete sulfidation of Ni_2P at 5.0 MPa hydrogen and 0.1 MPa H_2S. When the gas-phase PH_3 concentration is >0.1 ppm, the free energy change for the sulfidation of Ni_2P to Ni_3S_2 remains positive up to 825 K. This means that complete sulfidation of Ni_2P will not occur as long as a trace amount of PH_3 is present in the gas phase. The excess phosphorus, which is normally contained in fresh catalyst [17], can easily provide this trace amount of PH_3. Combining the results of Figs. 7 and 8, we conclude that at hydrotreating conditions, bulk Ni_2P is stable against complete sulfidation, but the surface layer can be partially (up to 50%) sulfided by sulfur replacement of phosphorus to create an overlayer with stoichiometry of Ni_3PS. This Ni_3PS surface stoichiometry is also consistent with the "PS" compound similar to Ph_3PS previously observed in XPS spectra of $NiPS_3$ [22].

3.3. CO adsorption

The adsorption of sulfur atoms at the TFH sites and the replacement of surface phosphorus by sulfur are thermodynamically favored processes for forming sulfur species on the (001) surface of Ni_2P at hydrotreating conditions. To determine which of these sulfur species can better represent the phosphosulfide structure, which has been proposed as the actual active

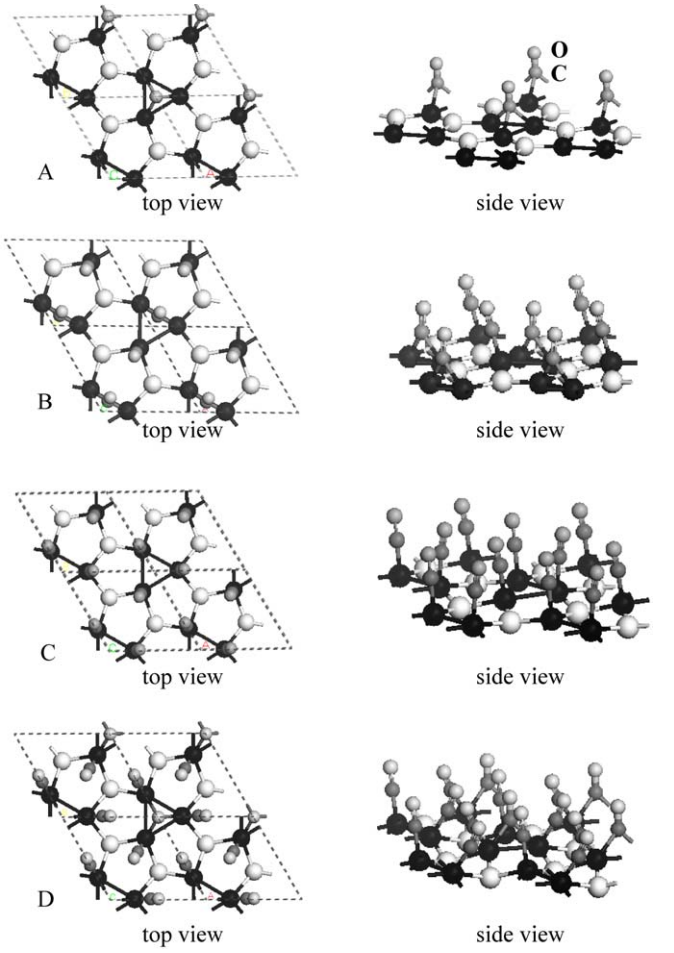

Fig. 9. Configurations of CO adsorption on the $Ni_2P(001)$ surface as a function of CO coverage: (A) 0.33 ML, with CO on the TFH site; (B) 0.67 ML, with one CO on the Ni–Ni bridge site and one terminally bonded to a single Ni site; (C) 1 ML, with one CO terminally bonded to one Ni site; (D) 1.33 ML, with one CO on the TFH site and three terminally bonded to Ni sites.

phase during hydrotreating [17–19], we further studied the adsorption of CO on the pristine Ni_3P_2 surface, as well as on the two types of surfaces with surface sulfur species.

The preferred configurations for CO adsorption on the Ni_3P_2 surface at different coverages are shown in Fig. 9. At low coverage, CO molecules preferentially occupy the nickel TFH sites (Fig. 9A). If monolayer (ML) adsorption is defined as one CO molecule per nickel site, then this low coverage corresponds to 0.33 ML. At 0.67 ML coverage, one CO molecule bridges two nickel atoms, and the other CO is linearly adsorbed on top of the other nickel site, as shown in Fig. 9B. At 1 ML coverage, each CO molecule linearly bonds to a nickel site (Fig. 9C). At 1.33 ML, four CO molecules are adsorbed on three nickel sites, one on the TFH site, each of the other three bonds linearly to one nickel site (Fig. 9D).

On the sulfur-replaced Ni_3PS surface, the adsorbed CO molecules adopt similar configurations as on the pristine Ni_3P_2 surface, but with lower adsorption energies. Table 1 summarizes the adsorption energies for CO adsorption on Ni_3P_2 and Ni_3PS surfaces at different coverages. At corresponding coverages, the adsorption energies of CO on the phosphorus-replaced Ni_3PS surface are always weaker than those on the pristine Ni_3P_2 surface. The adsorption of CO on the surface covered by adsorbed sulfur atoms is not energetically favored. Fig. 10 shows three possible configurations for CO on the sulfur-deposited surface. In Fig. 10A, CO is initially positioned to bond a nickel site; during geometry optimization, the CO forms bonds with both sulfur and nickel atoms with an adsorption energy of +0.07 eV. When a CO molecule is positioned at bridge site between Ni and P (Fig. 10B), the adsorption energy is +0.12 eV. The adsorption energy for a CO molecule on a P site is even higher; +0.38 eV (Fig. 10C). These results indicate that CO molecules cannot adsorb on the Ni_2P surface once the nickel sites are blocked by sulfur atoms.

Table 1
Adsorption energies of CO on the pristine $Ni_2P(001)$ surface (on the Ni_3P_2 surface) and the 50% phosphorus-replaced surface (on the Ni_3PS surface) at different coverages

Coverage (ML)	Adsorption energy (eV/CO)	
	On Ni_3P_2	On Ni_3PS
0.33	−1.97	−1.79
0.67	−1.25	−1.04
1.00	−1.05	−0.91
1.33	−0.40	−0.31

Layman and Bussell reported that the adsorption enthalpies of CO on the reduced and sulfided Ni_2P/SiO_2 catalyst are −31.4 and −30.5 kJ mol^{-1}, respectively [18]. These data are very close to the present calculated data at 1.33 ML coverage (Table 1; 38.3 and 30.3 kJ mol^{-1} for the Ni_3P_2 and Ni_3PS surfaces, respectively). Based on the experimental method, the adsorption enthalpies that they measured reflect only the binding strengths of linearly bonded CO molecules. According to the calculation data, the energies required for reducing CO coverage from 1 to 0.33 ML are 56.7 and 44.6 kJ mol^{-1} for the Ni_3P_2 and Ni_3PS surfaces, respectively. More importantly, the general trend revealed by the calculated data agrees very well with the experimental observations, whereby CO adsorbs slightly more strongly on the reduced Ni_2P surface than on the partially sulfided surface [18]. On the other hand, when the nickel sites are blocked by sulfur, the adsorption of CO on the surface is an endothermic process (Fig. 10). These energetic data suggest that the sulfur replacement model can better describe the structure of partially sulfided Ni_2P that is stable at hydrotreating reactions.

We further calculated the vibrational frequencies of adsorbed CO on the Ni_3P_2 and Ni_3PS surfaces; the results are presented in Table 2. For 0.33 ML CO coverage, only one CO molecule is adsorbed on the TFH site. The frequencies for the C–O stretching of CO bonded to the TFH site are 1831 cm^{-1} on the Ni_3P_2 surface (Fig. 9A) and 1849 cm^{-1} on the Ni_3PS surface. For 0.67 ML CO coverage, there are two adsorbed CO molecules; one adsorbs at a Ni–Ni bridge site, and the other is terminally bonded to a single nickel site (Fig. 9B). The frequency at 2074 cm^{-1} on the Ni_3P_2 surface and the frequency at 2087 cm^{-1} on the Ni_3PS surface are due to the stretching vibration of the terminally bonded CO. The lower frequencies of 1864 and 1813 cm^{-1} for the 0.67 ML coverage on the Ni_3P_2

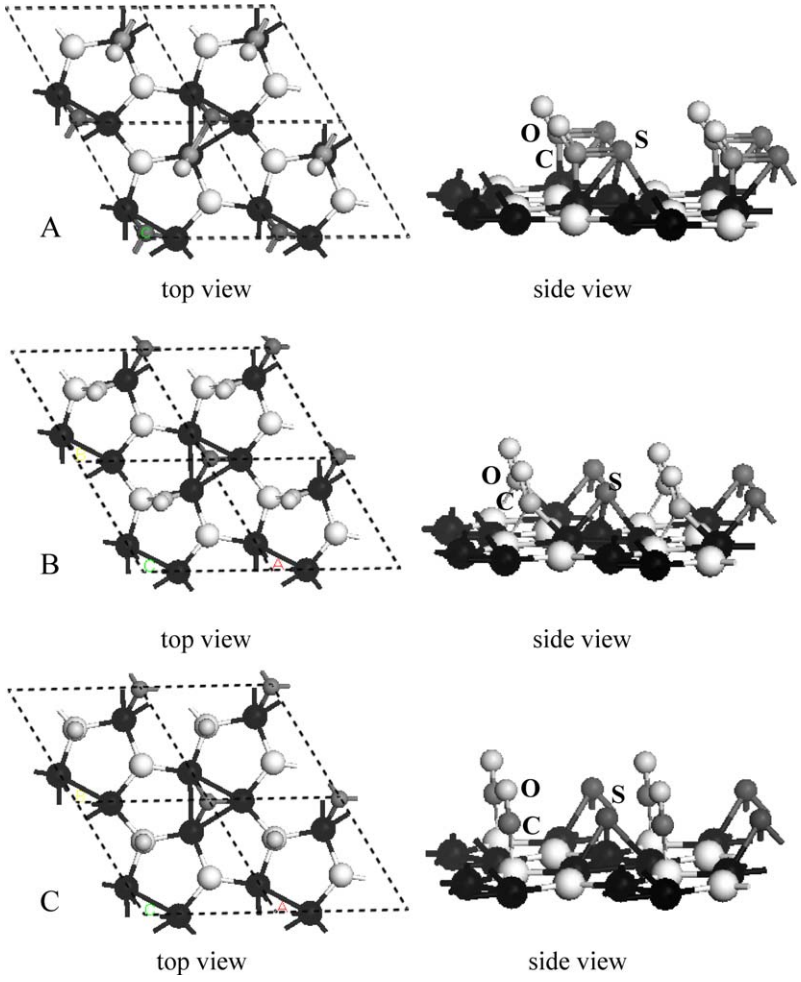

Fig. 10. Configurations of CO adsorption on the $Ni_2P(001)$ surface with the TFH site occupied by an adsorbed sulfur atom: (A) CO bonds nickel and sulfur; (B) CO bonds to nickel and phosphorus; (C) CO bonds to phosphorus.

Table 2
Calculated vibrational frequencies (cm^{-1}) of adsorbed CO on the pristine $Ni_2P(001)$ surface (on the Ni_3P_2 surface) and the 50% phosphorus-replaced surface (on the Ni_3PS surface) at different coverages

Coverage (ML)	Vibrational frequency (cm^{-1})	
	On Ni_3P_2	On Ni_3PS
0.33	1831	1849
0.67	2074, 1864	2087, 1813
1.00	2087, 1997, 1985	2091, 2004, 1972
1.33	2088, 2015, 2012, 1727	2090, 2025, 2011, 1719

and the Ni_3PS surfaces, respectively, are due to the stretching of the bridge CO molecules. For the 1 ML coverage, each CO molecule terminally bonds to one nickel site on both Ni_3P_2 and Ni_3PS surfaces (Fig. 9C). The symmetric stretching of the three CO molecules produces frequencies of 2087 and 2091 cm^{-1} on the Ni_3P_2 and Ni_3PS surfaces, respectively; asymmetric stretching results in lower frequencies of 1997 and 1985 cm^{-1} on the Ni_3P_2 surface and 2004 and 1972 cm^{-1} on the Ni_3PS surface. For 1.33 ML CO coverage, one CO molecule sits on the TFH site, and three other CO molecules are terminally bonded to nickel sites on both Ni_3P_2 and Ni_3PS surfaces (Fig. 9D). The symmetric stretching of the three terminally bonded CO molecules produces frequencies of 2088 and 2090 cm^{-1} on the Ni_3P_2 and Ni_3PS surfaces, respectively; asymmetric stretching of the terminally bonded CO molecules results in frequencies of 2015 and 2012 cm^{-1} on the Ni_3P_2 surface and 2025 and 2011 cm^{-1} on the Ni_3PS surface. CO at the TFH site has a vibrational frequency of 1727 cm^{-1} on the Ni_3P_2 surface and 1719 cm^{-1} the Ni_3PS surface. The shift of the TFH CO vibrational frequency at 1.33 ML to a lower frequency compared with that at 0.33 ML CO coverage is due to interference arising from the three neighboring linearly bonded CO molecules, which are not present at 0.33 ML.

The foregoing results indicate a general trend of the replacement of phosphorus by sulfur on the $Ni_2P(001)$ surface shifting the frequency of terminally bonded CO on nickel sites to a higher value by 2–13 cm^{-1} depending on CO coverage (Table 2). Layman and Bussell [18] observed a strong absorbance at about 2083 cm^{-1} in their IR spectra for CO adsorbed on the reduced Ni_2P/SiO_2 sample, which was attributed to the terminally bonded CO on nickel sites. On the sulfided Ni_2P/SiO_2, the frequency shifted to 2093 from 2083 cm^{-1}. Similar observations were also reported by Sun et al. [19]; the frequency of CO adsorbed on reduced Ni_2P/SiO_2 was 2082 cm^{-1}, and shifted to 2094 cm^{-1} on a H_2S/H_2-treated sample. These experimental re-

sults are in excellent agreement with our calculated data based on the sulfur replacement model (Table 2). The sulfidation not only shifted the CO stretching frequency, but also dramatically decreased the intensity of the absorbance for the terminally bonded CO molecules on nickel sites [18,19], which cannot be explained by the sulfur replacement model. It has been shown that CO cannot adsorb on the surface where the TFH sites are blocked by adsorbed sulfur atoms. We have also found that both sulfur adsorption on the TFH sites and sulfur replacement of surface phosphorus are thermodynamically favored processes. In addition, calculating the energy change for sulfur adsorption on the TFH sites on the phosphorus-replaced Ni_3PS surface revealed that sulfur replacement weakens the sulfur–TFH interaction by 0.25 eV/S. Therefore, these two processes might have occurred simultaneously on the Ni_2P catalyst surface in the presence of H_2S and hydrogen at high temperatures. This would explain why sulfidation could shift the frequency of adsorbed CO and also significantly reduce the intensity of absorbance.

Combining the calculation results and the literature experimental observations [18,19], we propose that the sulfur replacement Ni_3PS plus sulfur deposition surface is a consistent model for the so-called "phosphosulfide" phase, which is believed to be the actual active phase for Ni_2P catalyst at hydrotreating conditions. The formation of deposited sulfur at TFH sites, which would block the adsorption sites for CO and other molecules, would not be beneficial for hydrotreating reactions. The phosphorus-replaced surface with open TFH sites would be an ideal structure for hydrotreating reactions. Based on results of the present work, further studies on hydrogen dissociation, adsorption, and reactions of sulfur- and nitrogen-containing molecules on Ni_2P catalyst should consider the partially sulfided Ni_3PS surface, possibly with additional atomic sulfur at TFH sites, as the model of the actual active phase of Ni_2P at hydrotreating reactions.

4. Conclusion

Bulk Ni_2P is stable against complete sulfidation at normal hydrotreating conditions, but up to 50% surface phosphorus could be replaced by sulfur in the presence of gas-phase H_2S and H_2. It is also energetically favorable for H_2S to adsorb and dissociate on the pristine Ni_2P and phosphorus-replaced Ni_3PS surface. The adsorption energy of CO on the sulfur replacement surface is slightly lower that on the pristine (001) surface of Ni_2P. The calculated frequencies of IR absorbance for terminally bonded CO are about 2–13 cm^{-1} higher on the sulfur replacement surface (Ni_3PS) than that on the pristine (001) surface of Ni_2P. Based on our calculations combined with experimental observations reported in the literature, we conclude that the 50% phosphorus-replaced surface (i.e., Ni_3PS, with deposited sulfur atoms on the TFH sites) is a reasonable representation for the actual active phase of Ni_2P at hydrotreating reactions.

Acknowledgment

This work is supported by the Natural Sciences and Engineering Research Council (NSERC) Discovery Grant program.

References

[1] R. Prins, V.H.J. de Beer, G.A. Somorjai, Catal. Rev.-Sci. Eng. 31 (1989) 1.
[2] H. Topsøe, B.S. Clausen, F.E. Massoth, in: J.R. Anderson, M. Boudart (Eds.), Hydrotreating Catalysis, in: Science and Technology, vol. 11, Springer, Berlin, 1996.
[3] S. Cristol, J.F. Paul, E. Payen, D. Bougeard, S. Clémendot, F. Hutschka, J. Phys. Chem. B 104 (2000) 11220.
[4] R. Prins, Adv. Catal. 46 (2001) 399.
[5] H. Schweiger, P. Raybaud, G. Kresse, H. Toulhoat, J. Catal. 207 (2002) 76.
[6] M. Sun, D. Nicosia, R. Prins, Catal. Today 86 (2003) 173.
[7] T.C. Ho, Catal. Today 98 (2004) 3.
[8] H. Topsøe, B. Hinnemann, J.K. Nørskov, J.V. Lauritsen, F. Besenbacher, P.L. Hansen, G. Hytoft, R.G. Egeberg, K.G. Knudsen, Catal. Today 107 (2005) 12.
[9] P. Clark, W. Li, S.T. Oyama, J. Catal. 200 (2001) 140.
[10] C. Stinner, R. Prins, Th. Weber, J. Catal. 202 (2001) 187.
[11] D.C. Phillips, S.J. Sawhill, R. Self, M.E. Bussell, J. Catal. 207 (2002) 266.
[12] C. Stinner, Z. Tang, M. Haouas, Th. Weber, R. Prins, J. Catal. 208 (2002) 456.
[13] S.T. Oyama, X. Wang, Y.-K. Lee, K. Bando, F.G. Requejo, J. Catal. 210 (2002) 207.
[14] S.T. Oyama, X. Wang, F.G. Requejo, T. Sato, Y. Yoshimura, J. Catal. 209 (2002) 1.
[15] S.T. Oyama, J. Catal. 216 (2003) 343.
[16] V. Zuzaniuk, R. Prins, J. Catal. 219 (2003) 85.
[17] S.T. Oyama, X. Wang, Y.-K. Lee, W.-J. Chun, J. Catal. 221 (2004) 263.
[18] K.A. Layman, M.E. Bussell, J. Phys. Chem. B 108 (2004) 10930.
[19] F. Sun, W. Wu, Z. Wu, J. Guo, Z. Wei, Y. Yang, Z. Jiang, F. Tian, C. Li, J. Catal. 228 (2004) 298.
[20] S. Yang, C. Liang, R. Prins, J. Catal. 237 (2006) 118.
[21] W.R.A.M. Robinson, J.N.M. van Gestel, T.I. Koranyi, S. Eijsbouts, A.M. van der Kraan, J.A.R. van Veen, V.H.J. de Beer, J. Catal. 161 (1996) 539.
[22] T.I. Koranyi, Appl. Catal. A 239 (2003) 253.
[23] R.W.G. Wyckoff, Crystal Structures, vol. 1, Interscience Publishers, New York, 1963.
[24] M.G. Moula, S. Suzuki, W.J. Chun, S. Otani, S.T. Oyama, K. Asakura, Chem. Lett. 35 (2006) 90.
[25] P. Liu, J.A. Rodriguez, T. Asakura, J. Gomes, K. Nakamura, J. Phys. Chem. B 109 (2005) 4575.
[26] B. Delley, J. Chem. Phys. 113 (2000) 7756.
[27] A.D.J. Becke, Chem. Phys. 88 (1988) 2547.
[28] J.P. Perdew, Y. Wang, Phys. Rev. B 45 (1992) 13244.
[29] M. Dolg, U. Wedig, H. Stoll, H. Preuss, J. Chem. Phys. 86 (1987) 866.
[30] A. Bergner, M. Dolg, W. Kuechle, H. Stoll, H. Preuss, Mol. Phys. 80 (1993) 1431.
[31] M. Sun, A.E. Nelson, J. Adjaye, J. Catal. 226 (2004) 32.
[32] P. Raybaud, J. Hafner, G. Kresse, S. Kasztelan, H. Toulhoat, J. Catal. 189 (2000) 129.
[33] M.V. Bollinger, K.W. Jacobsen, J.K. Nørskov, Phys. Rev. B 67 (2003) 85410.